On the Mechanism of Actin Monomer-Polymer Subunit Exchange at Steady State*

Stephen L. Brenner‡ and Edward D. Korn§

From the ‡Office of the Director, Division of Computer Research and Technology, and the §Laboratory of Cell Biology,
National Heart, Lung, and Blood Institute, National Institutes of Health, Bethesda, Maryland 20205

The rate of exchange of G-actin with subunits of F-actin and the rate of hydrolysis of ATP in solutions of F-actin at steady state have been measured simultaneously. Subunit exchange kinetics were analyzed by both a treadmill model and an exchange-diffusion model. The best fit to a treadmill model of the data obtained in 0.5 mM MgCl₂ and 0.2 mM ATP at 30 °C gave a treadmill efficiency (net monomers incorporated per ATP hydrolyzed) of 0.26, in good agreement with the previously reported s-value of 0.25 (Wegner, A. (1976) J. Mol. Biol. 108, 139-150) for similar ionic conditions. However, in this and other conditions with excess free divalent cations (Ca^{2+} or Mg^{2+}), the observed exchange kinetics were in better agreement with an exchange-diffusion model than with a treadmilling model over the entire time course of the experiment. In the absence of excess divalent cations (50 mM KCl), exchange was too slow to be analyzed adequately by either model. Using the measured filament length distribution and the observed fit of the exchange-diffusion model to the data in 0.5 mM MgCl₂, an on-rate constant of 2.8 × 10⁶ $M^{-1} s^{-1}$ and an off-rate constant of 5.8 s^{-1} were calculated. These values, while in good agreement with previously measured pre-steady state polymerization rate constants under different ionic conditions (Pollard, T. D., and Mooseker, M. S. (1981) J. Cell Biol. 88, 654-659), are about 30-fold higher than the rate constants predicted from the rate of ATP hydrolysis at steady state. To rationalize these discrepancies, a model is proposed in which a segment of F-actin subunits at one or both ends of the filament contains bound ATP at steady state.

Actin polymerization in the presence of ATP is accompanied by the hydrolysis of G-actin-bound ATP yielding F-actin with predominantly, if not exclusively, bound ADP. The kinetics of polymerization under a variety of ionic conditions have been successfully modeled by a nucleation-elongation reaction (1-3). Once polymerization is complete, a pool of monomeric actin (at the critical concentration) co-exists at steady state with polymeric F-actin and the hydrolysis of ATP continues due, at least in part, to assembly-disassembly reactions at the filament ends.

The actin filament has two structurally and kinetically distinct ends called barbed (B) and pointed (P) from the arrowhead pattern seen when actin is decorated with muscle heavy meromyosin. In the simplest polymerization model, the only reactions that occur during elongation and at steady state are the addition of G-ATP actin monomers to F-ADP actin filaments, with the concomitant hydrolysis of ATP, and the loss of G-ADP monomers from filament ends, followed by much more rapid exchange of actin-bound ADP for free ATP. In this case, the description of the actin filament elongation reaction and the steady state assembly-disassembly reaction requires specification of only four rate constants: the on-rate constants (k_B^+ and k_P^+) and the off-rate constants (k_B^- and k_P^-) at each filament end.[1] In an equilibrium system (when ATP is not hydrolyzed or when only G-ADP actin is present) the two ends of the actin filament must have equal critical concentrations so that $A_{1B} = k_B^-/k_B^+$ must equal $A_{1P} = k_P^-/k_P^+$ which equals A_1, the measured critical concentration.

Wegner (7) was the first to point out that when ATP is hydrolyzed in a solution containing F-actin and G-actin at steady state, the on- and off-reactions at each filament end are not symmetrical, i.e. ATP is hydrolyzed in the association reaction but ATP is not synthesized in the dissociation reaction. Therefore, neither filament end is at equilibrium although the system is at steady state. Thus, the two ends of an actin filament can have different critical concentrations with the observed critical concentration, $A_1 = (k_B^- + k_P^-)/(k_B^+ + k_P^+)$, lying between the two. As a result, there will be continual net loss of monomeric actin from the high critical concentration end, balanced by continual net addition of monomers to the low critical concentration end. Previous studies of the action of a variety of actin binding factors that appear to cap one or the other end of the filament (5) have provided indirect evidence for different critical concentrations at the two filament ends (in the presence of ATP) and data on actin-monomer-polymer subunit exchange at steady state have been analyzed to provide evidence for an actin treadmill (7, 8).

Subunit exchange between monomer and polymer can also occur by random fluctuations in the lengths of an ensemble of polymers. This exchange-diffusion mechanism (9) (which can be unidirectional or bidirectional depending on whether one or both filament ends are involved (7)) is the only mechanism for subunit exchange when the two filament ends have the same critical concentration which, it is important to note, can happen even when ATP is being hydrolyzed. In the context of

---

[1] If ATP hydrolysis is not obligatory to monomer addition (4, 5) or if a substantial portion of the G-actin pool contains bound ADP instead of ATP (6), additional reactions (and associated rate constants) must be included for the addition and dissociation of G-ATP actin without hydrolysis of ATP, the addition of G-ADP actin, the exchange of ATP for ADP on G-actin (cf. Ref. 6, and, possibly, the hydrolysis of filament-bound ATP.

the simple model described above, both exchange-diffusion and treadmilling will occur when the critical concentrations at the two ends of the filaments are different. For exchange-diffusion to dominate when both exchange mechanisms occur, however, the magnitude of the rate constants at one filament end must be very much greater than at the other end.

We have now used a sensitive fluorescence assay (10) to study the kinetics of monomer-polymer subunit exchange under a variety of ionic conditions, including excess free Mg^{2+} (where from previous observations the critical concentrations at the two filament ends are expected to differ (11, 12)) and KCl with no free Mg^{2+} (where the critical concentrations at the two filaments ends may be the same (13)). Simultaneous measurements of the rates of steady state ATP hydrolysis were also made. Under all conditions studied, the time course of subunit exchange was more consistent with an exchange-diffusion mechanism than with a treadmill model. More extensive analysis of the data obtained in 0.5 mM $MgCl_2$ and 0.2 mM ATP at 30 °C suggests that F-actin may contain a segment of subunits with bound ATP at, at least, one end of the filament.

MATERIALS AND METHODS

N-Pyrenyliodoacetamide from Molecular Probes was used without further purification. ATP was from Sigma. [γ-^{32}P]ATP (2–10 Ci/mmol) from New England Nuclear was diluted immediately upon arrival to 0.5–1.0 mCi/ml in 2 mM ATP and stored at −20 °C. Procedures to determine the radiochemical purity and concentration of ATP solutions were previously described (14).

Muscle G-actin was prepared from acetone powders of rabbit back and leg muscle by the method of Spudich and Watt (15), as modified by Eisenberg and Kielley (16), followed by gel filtration on Sephadex G-200. Monomeric actin was stored on ice in a buffer containing 5 mM Tris·HCl, 0.2 mM dithiothreitol, 0.2 mM ATP, 0.1 mM $CaCl_2$, and 0.01% NaN_3, pH 8.0 (buffer G). The concentration of monomeric actin was determined either from its absorbance at 290 nm, using an extinction coefficient of 0.617 mg^{-1} ml cm^{-1} (17), or by the procedure of Lowry *et al.* (18) using muscle G-actin as a standard.

G-actin was labeled with [γ-^{32}P]ATP, and the bound nucleotide (0.95–1.03 mol of ATP/mol of actin) and total exchangeable nucleotide (typically > 0.93 mol of ATP/mol of actin) were determined as described previously (19). Hydrolysis of [γ-^{32}P]ATP was followed by measuring the release of ^{32}P$_i$ (20).

Pyrenyl actin[2] was prepared by reacting actin with *N*-pyrenyliodoacetamide using a modification of the procedure of Kouyama and Mihashi (10). G-actin (40 mg, 2 mg/ml) was polymerized at 25 °C for 1 h in 5 mM Tris·HCl, 0.1 M KCl, 2 mM $MgCl_2$, 0.1 mM $CaCl_2$, 0.5 mM ATP, 0.1 mM dithiothreitol, 0.01% NaN_3, and then dialyzed overnight at 4 °C against this same buffer. A 0.20-ml aliquot of freshly prepared *N*-pyrenyliodoacetamide in dimethyl formamide (14 mg/ml) was added to the F-actin, and the solution was mixed by inversion and incubated overnight at 20 °C with occasional mixing. The reaction was quenched by adding 0.05 ml of 0.2 M dithiothreitol. Excess unreacted insoluble dye was removed by centrifugation at 2,500 × g for 15 min and the labeled F-actin pelleted at 29,000 rpm (Type 30 rotor) for 3½ h at 20 °C. The pellet was homogenized in 5 ml of buffer G, dialyzed for 72 h *versus* several changes of buffer G, clarified at 40,000 rpm (Type 40 rotor) for 2 h at 4 °C, and applied directly to a Sephadex G-200 column (78 × 1.6 cm) at 4 °C with a flow rate of 8–10 ml/h. Peak tubes were pooled and the actin concentration was determined by the procedure of Lowry et al. (18). The extent of labeling was determined using an extinction coefficient of 2.2 × 10^4 M^{-1} cm^{-1} at 344 nm (10). The actin typically contained 0.98–1.02 mol of label/mol of actin.

Electron microscopy was used to determine the actin filament length distributions. Experimental samples (0.5 mg/ml of actin) were applied directly to inverted carbon-coated Formvar grids and stained with 1% uranyl acetate as described elsewhere (21). Photographs were taken using a Siemens Elmiskop electron microscope and filament lengths determined at a final magnification of 18,750 using a Summa Graphics ID digitizer.

[2] The trivial name used is: pyrenyl actin, *N*-pyrenylcarboxyamidomethyl actin.

Polymerization and steady state monomer-polymer exchange measurements were made using an SLM 4000 spectrofluorometer with the sample chamber thermostatted at 30 °C. All measurements were made on 0.4-ml samples in quartz cuvettes (3 × 10 mm) (Precision Cells) with the long dimension of the cell parallel to the incoming light path. For 90° light scattering experiments, the excitation and emission wavelengths were 450 nm and the excitation and emission bandpasses were 2 nm. For fluorescence measurements on pyrenyl actin, the excitation and emission wavelengths were 368 and 388 nm and the respective bandpass settings were 1 and 4 nm. No light scattering signal could be detected at 388 nm when unlabeled F-actin was exposed to light at 368 nm. To avoid bleaching the fluorophore, pyrenyl actin was prepared and stored in the dark and, during fluorescence experiments, was exposed to the light source only intermittently.

Critical actin concentrations were determined by first polymerizing 20 μM actin (5% pyrenyl actin) at 30 °C, then diluting in the same buffer to multiple lower actin concentrations. After a 16- to 20-h incubation in the dark at 30 °C, both the steady state fluorescence and light scattering of each sample were measured.

RESULTS

The results of the monomer-polymer subunit exchange experiments were analyzed using two distinct models, treadmilling and exchange-diffusion. In order to facilitate comparison of the models, first the experimental data are presented and then the data are analyzed according to the models, which are developed in the "Appendix."

Experimental Observations

Actin Polymerization and Associated ATP Hydrolysis— G-actin, 5% labeled with *N*-pyrenyliodoacetamide, was equilibrated in buffer G containing 0.2 mM [γ-^{32}P]ATP, polymerization was initiated at 30 °C by the addition of 0.5 mM $MgCl_2$, and the polymerization kinetics were monitored by both light scattering and fluorescence (Fig. 1). In other experiments, it was found that these two assays gave indistinguishable results over a range of concentrations of pyrenyl actin (0.2–6% of the total actin) and a variety of ionic conditions (50–100 mM KCl, 0.5–2.0 mM $MgCl_2$, 1–2 mM $CaCl_2$). In addition, Fig. 2 shows that the critical concentrations determined by fluorescence, under several ionic conditions, were identical with those found by light scattering. We conclude, therefore, in agreement with others (10, 22, 23), that pyrenyl actin co-polymerizes with
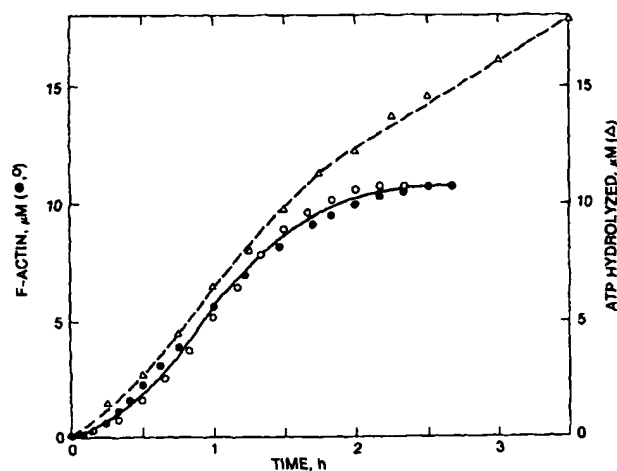

FIG. 1. **Actin polymerization and associated ATP hydrolysis in 0.5 mM $MgCl_2$.** G-actin (12.1 μM, 5% pyrenyl actin) equilibrated in buffer G containing 0.22 mM [γ-^{32}P]ATP was polymerized at 30 °C by addition of 0.5 mM MgC_2. Polymerization was monitored by either light scattering (O) or fluorescence (●) as described under "Materials and Methods." Simultaneous measurements of ATP hydrolysis (Δ) were made.

FIG. 2. Actin critical concentrations. F-actin (20 μM, 5% pyrenyl actin) in buffer G containing 0.5 mM MgCl₂ (*A*), 50 mM KCl (*B*), or 20 mM KCl, 0.5 mM MgCl₂ (*C*) was diluted to multiple actin concentrations in the corresponding buffers and incubated for 16–20 h at 30 °C. Both the final fluorescence (●) and light scattering (○) were measured. The critical concentrations were 1.4 μM (*A*), 0.7 μM (*B*), and 0.5 μM (*C*). In 0.5 mM MgCl₂, the measured critical concentration varied from 1.4 to 2.1 μM for different actin preparations; values obtained from light scattering measurements always agreed with those obtained from fluorescence measurements.
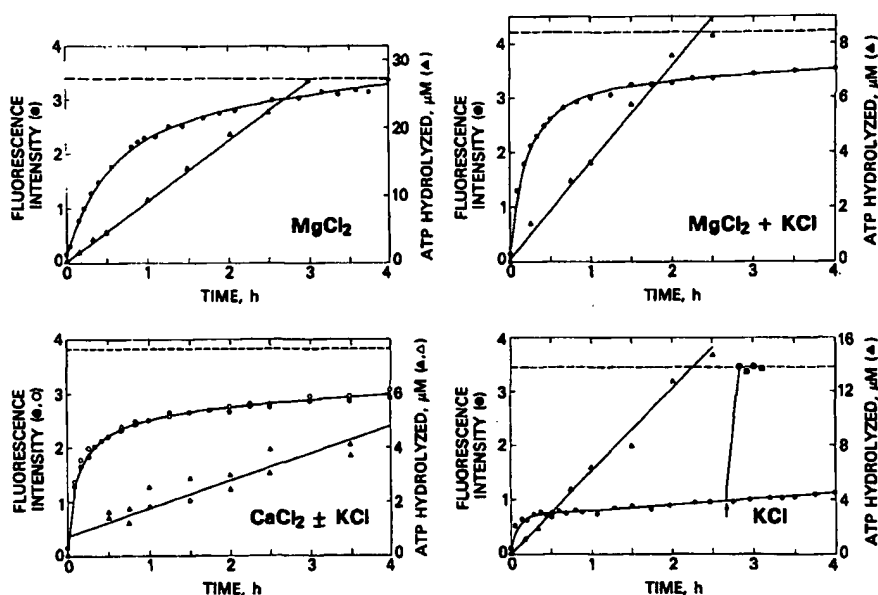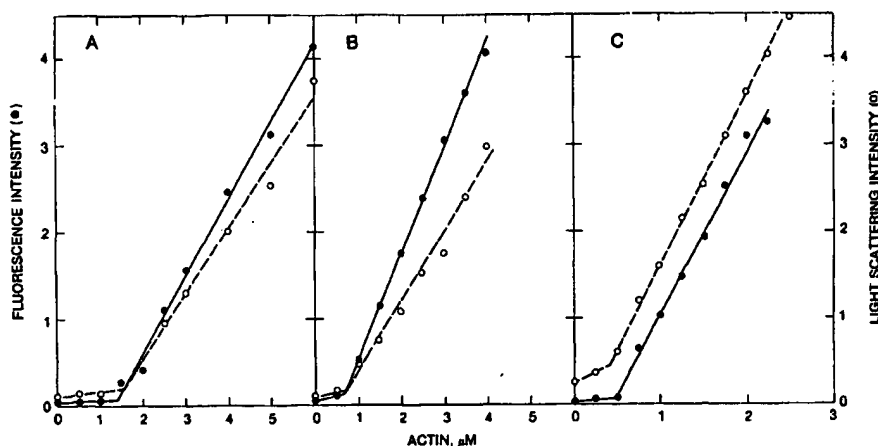

FIG. 3. Incorporation of G-actin into F-actin and hydrolysis of ATP at steady state. G-actin (12 μM), equilibrated in buffer G containing 0.23 mM [γ-³²P]ATP, was polymerized to steady state at 30 °C by addition of either 0.5 mM MgCl₂ (*upper left*), 0.5 mM MgCl₂ + 20 mM KCl (*upper right*), 2 mM CaCl₂ (*lower left*, ●, ▲), 2 mM CaCl₂ + 20 mM KCl (*lower left* ○, △), or 50 mM KCl (*lower right*). The critical concentrations for these samples were 2.1, 0.5, 0.6, 0.6, and 0.5 μM, respectively. Pyrenyl G-actin (1–2 μl) was added to 2 ml of each F-actin solution. The final pyrenyl actin concentration was 0.08 μM in the MgCl₂ experiment and 0.04 μM in all other experiments. After gentle mixing by inversion, 0.4-ml aliquots were transferred to a quartz curvette (3 × 10 mm) and the fluorescence was monitored as described under "Experimental Procedures" (●, ○). Simultaneous measurements of the rate of ATP hydrolysis were made (▲, △). For each ionic condition, a sample of G-actin was co-polymerized with pyrenyl G-actin to determine the final fluorescence at equilibrium (*dashed line*). At the time indicated by the *arrow*, the sample in 50 mM KCl (*lower right*) was subjected to sonication for 5 s at setting 3 on a Heat Systems Ultrasonic Sonifier, and the fluorescence was measured (■). The *lines* drawn through the *points* are not theoretical fits.

unmodified actin and that the increase in fluorescence of pyrenyl actin monitors G-actin subunit incorporation into F-actin.

Simultaneous measurements of ATP hydrolysis (Fig. 1) showed that, during polymerization in 0.5 mM MgCl₂, ATP was hydrolyzed as fast as monomers were incorporated into polymers. In the experiment shown, when polymerization was complete, slightly more than one molecule of ATP had been hydrolyzed for each F-actin protomer. Similar results were obtained under a variety of ionic conditions (50–100 mM KCl, 0.5–2.0 mM MgCl₂, 1–2 mM CaCl₂).

Actin Monomer-Polymer Subunit Exchange and ATP Hydrolysis at Steady State—As shown in Fig. 1, hydrolysis of ATP by actin continues after polymerization is complete. To

examine the relationship between this ATPase activity and monomer-polymer subunit exchange, G-actin, equilibrated with 0.2 mM [γ-³²P]ATP, was polymerized to steady state at 30 °C by addition of various salts (Fig. 3). Simultaneous measurements of steady state ATP hydrolysis and actin exchange were made by adding trace amounts of pyrenyl actin to the solutions of F-actin at steady state, gently mixing, and monitoring the release of ³²Pᵢ and the increase in fluorescence as labeled monomers were incorporated into polymers.

As shown in Fig. 3, ATP hydrolysis occurred at a constant rate for the duration of the experiments. Except perhaps in CaCl₂ ± KCl (Fig. 3, *lower left*), where the ATPase rate was very low and difficult to measure precisely, there was no detectable burst of ATP hydrolysis upon mixing pyrenyl G-

actin with the steady state F-actin solution. This indicates that little, if any, ATP hydrolysis was associated with any transient filament breakage that might have occurred during mixing, followed by reannealing during the subsequent incubation. The ATPase rate varied from a low of about 1.0 μM/h in CaCl$_2$ $\pm$ KCl to a high of 9.0 μM/h in 0.5 mM MgCl$_2$.

Essentially complete fluorescence equilibrium was attained in about 4 h in 0.5 mM MgCl$_2$ (Fig. 3, *upper left*). In many different experiments, over a range of total actin concentrations (12–48 μM), greater than 95% fluorescence equilibrium was always observed within 4 h in the presence of 0.5 mM MgCl$_2$. Under the other ionic conditions examined, however, complete equilibration was never observed during the 4-h time course, even though the initial rate of fluoresence increase was often higher than in the presence of MgCl$_2$ alone.

Actin polymerized in 0.5 M MgCl$_2$ + 20 mM KCl (Fig. 3, *upper right*) had a lower critical concentration (0.5 M *versus* 2.1 μM), lower steady state ATPase rate (3.6 μM *versus* 9.0 μM/h), and higher initial rate of fluoresence increase than actin polymerized in 0.5 mM MgCl$_2$ alone. But, in the presence of MgCl$_2$ + KCl, the fluorescence curve was clearly biphasic and reached only 83% of the equilibrium fluorescence value in 4 h. On the other hand, in 2 mM CaCl$_2$, the rate of fluorescence increase, steady state rate of ATP hydrolysis, and the critical concentration were all unaffected by the presence of 20 mM KCl (Fig. 3, *lower left*). In CaCl$_2$ $\pm$ KCl, a rapid increase in fluorescence was followed by a very much slower phase that reached only 73% of the equilibrium fluorescence value in 4 h.

In the presence of 50 mM KCl and the absence of free divalent cations (Fig. 3, *lower right*), ATP hydrolysis at steady state occurred at a constant rate of 6.0 μM/h. After an initial burst, the fluorescence data indicated very slow exchange of actin monomers with polymers. There was no measureable burst in ATP hydrolysis corresponding to the initial burst in fluorescence. Rapid equilibration of pyrenyl monomer with F-actin was observed, however, following brief sonication.

Data Analysis

Fluorescence Increase and Turnover of F-Actin—At the beginning of experiments such as those described in Fig. 3, all of the pyrenyl actin is in the monomer pool. Net incorporation of G-actin into F-actin results in an increase in fluorescence but, as is developed more fully in the "Appendix," the fraction of F-actin that must turnover before the equilibrium fluorescence value is reached depends on the concentration of F-actin and the critical monomer concentration. As calculated from the total actin concentrations, the measured critical concentration, and Equation 7 (see "Appendix"), the per cent of F-actin filament subunits that had exchanged at the end of each of the experiments shown in Fig. 3 was at least 35% in MgCl$_2$, 8% in MgCl$_2$ + KCl, 7% in CaCl$_2$ $\pm$ KCl, and <2% in KCl alone. The near approaches to fluorescence equilibrium shown in Fig. 3, despite the low calculated turnover of the F-actin, result from the fact that, when the critical concentration is low compared to the concentration of F-actin, it requires very little monomer-polymer subunit exchange to incorporate most of the pyrenyl monomers into F-actin (see "Appendix"). As a result, the sensitivity of the assay is enhanced when the turnover rate is low, as in these experiments, allowing reliable data to be obtained.

Treadmilling Model—We show in the "Appendix" (Equation 11) that the treadmilling model for subunit exchange between pyrenyl G-actin and F-actin predicts a linear dependence of the term $-\ln (F(\infty) - F(t))$ with respect to time, where $F(\infty)$ is the fluorescence that would be observed if all the pyrenyl actin were in polymer and $F(t)$ is the observed fluorescence at any time, t. It can be seen in Fig. 4 (*open*
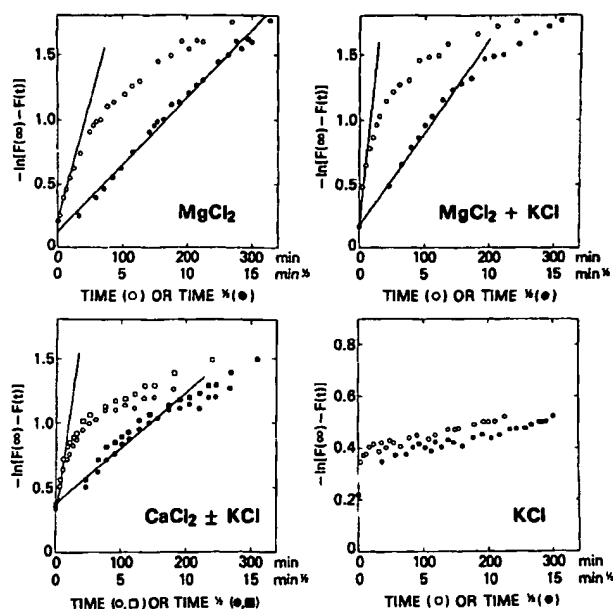

FIG. 4. **Analysis of steady state monomer-polymer subunit exchange kinetics: treadmill *versus* exchange-diffusion.** The fluorescence data in Fig. 3 are replotted according to the treadmill model (Equation 11 in "Appendix") (O, □) and the exchange-diffusion model (Equation 14 in "Appendix") (●, ■). The ionic conditions are given in the legend to Fig. 3. The *straight lines* are drawn through the *time points* that show the theoretical predicted linear dependence of $-\ln (F(\infty) - F(t))$ on time (treadmill model) or time$^{1/2}$ (exchange-diffusion model). In the *lower left*, the data for CaCl$_2$ + KCl (□, ■) and for CaCl$_2$ − KCl (O, ●) are plotted.

circles) that when the data in Fig. 3 are plotted in this way, they deviate significantly from the theoretical curves for the treadmilling model in all cases. In MgCl$_2$, the data were linear with time for only the first 20 min, in MgCl$_2$ + KCl for only 10–15 min, and in CaCl$_2$ $\pm$ KCl for <20 min of the total 4-h incubation period. In KCl alone, after an initial burst, very much slower exchange occurred than when excess free divalent cations were present.

There are two obvious reasons why the experimental data might fall below the theoretical curves if subunit exchange were, in fact, occurring by the treadmilling mechanism. First, there might have been a large increase in filament ends caused by fragmentation when the pyrenyl G-actin was mixed with the solution of F-actin at steady state followed by reduction in the number of filament ends by reannealing. The rate of ATP hydrolysis, however, was constant throughout the entire time courses of the incubations (Fig. 3). Since the ATPase rate is almost certainly proportional to the number of filament ends, it, therefore, seems very unlikely that the decrease in the apparent treadmilling rate can be explained by formation and loss of filament ends by fragmentation and reannealing.

Alternatively, the decrease in apparent treadmilling rates might have been due to the expected heterogeneity in filament lengths. In principle (see "Appendix"), short filaments would equilibrate relatively rapidly with the monomer pool, and their continued turnover after equilibration would not contribute to the increase in fluorescence. To determine if this could explain the poor fit of the experimental data to the theoretical treadmilling curve, the distribution of filament lengths was measured for the experiment in MgCl$_2$, the one for which the best fit to the treadmilling model was obtained to the highest fractional turnover of filament subunits. By combining the data for filament length distribution (Fig. 5)
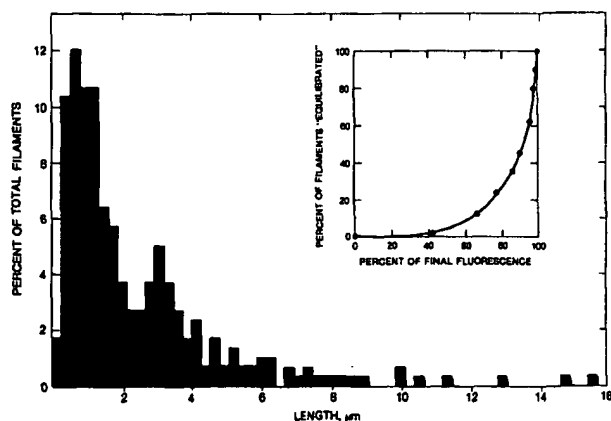
FIG. 5. **Filament length distribution of F-actin in 0.5 mM MgCl₂.** G-actin (12 μM) in buffer G was polymerized at 30 °C for 3 h by addition of 0.5 mM MgCl₂. After the sample was gently agitated (in the same way as when pyrenyl G-actin was added in the subunit exchange experiments described in the legend to Fig. 3), the filament length distribution was determined as described under "Materials and Methods." A total of 301 filaments were measured; the average filament length was 2.4 μm. The per cent of filaments which would have exchanged all of their subunits with the monomer pool was calculated as a function of the per cent of the final fluorescence (*inset*).

with Equation 8 (see "Appendix"), the per cent of filaments which had exchanged all of their subunits could be calculated as a function of the final fluorescence (Fig. 5, *inset*). Filaments that are calculated to have exchanged all their subunits are considered to have reached fluorescence equilibrium. It can be seen from Fig. 5 (*inset*), for example, that only 20% of the filaments would have reached fluorescence equilibrium when as much as 60–80% of the maximum fluorescence signal had been reached. As shown in Figs. 3 and 4, however, in the actual experiment, the apparent treadmilling rate had already dropped to about 50% of its initial value by about 30 min, at which time only about 30–40% of the equilibrium fluorescence had been reached. From the measured filament length distribution (Fig. 5), at this level of fluorescence essentially all of the filaments should still have been treadmilling and not until 90% of the final fluorescence value had been attained would the apparent treadmilling rate have decreased to 50%.

From the above considerations, then, it seems that neither transient filament breakage and reannealing nor completion of a treadmilling cycle by a portion of the F-actin filaments can explain the deviation of the experimental data from the time dependence predicted by Equation 11 (see "Appendix"). Therefore, the treadmilling model can be fit to the data for monomer-polymer exchange only for a very short period at the beginning of the experiments and, thus, this model does not seem to provide an adequate explanation for most of the experimental results.

Exchange-Diffusion Model—In contrast to the linear time dependence of the treadmilling model, the exchange-diffusion model for subunit exchange between pyrenyl G-actin and F-actin predicts a linear dependence of $-\ln((F(\infty) - F(t))$ with respect to $t^{1/2}$ (see "Appendix", Equation 14). As can be seen in Fig. 4 (*solid circles*), the experimental data in Fig. 3 appear to be much more consistent with the exchange-diffusion model than with the treadmilling model. In MgCl₂, the fluorescence data fit the $t^{1/2}$ dependence for nearly the entire time course of the experiment (more than 5 h). In MgCl₂ + KCl, the fit is good to 8–10 min$^{1/2}$ (*i.e.* 64–100 min) and, in CaCl₂ ± KCl, the fit is also good for about 100 min. The experimental data do fall below the theoretical curves at longer times in these latter two experiments but the fits appear to be very much better

than for the treadmilling model. In KCl alone, the data are not fit particularly well by either model but, because of the very slow rate of subunit exchange, very few data are available.

DISCUSSION

Our kinetic data for monomer-polymer subunit exchange in solutions of F-actin at steady state seem to be fit very much better by the exchange-diffusion model than by the treadmilling model, even for experiments in MgCl₂ where we expect the two filament ends to have different critical concentrations (11, 12). On the other hand, Wegner (7) and Wegner and Neuhaus (8) have successfully fit their exchange data, which were obtained from conceptually similar experiments using radiolabeled actin monomer, to a treadmilling model. Our data cannot be better rationalized with the treadmilling model by invoking fragmentation and reannealing because the ATPase rate was constant throughout the experiment as would not have been expected had the concentration of filament ends been changing significantly. We have also shown by direct measurement that no significant error is introduced into our calculations, at least for the experiment in MgCl₂, by the distribution of filament lengths. We have been unable to perform a similar analysis for the experiments in KCl because the filaments were entangled in large clumps making it impossible to determine their lengths by electron microscopy. The complete formulation of Wegner (7) also accounts for variations in filament lengths but does so implicitly by analysis of the polymerization kinetics rather than by direct measurement. Uncertainty about some of the assumptions of the polymerization model may limit that approach. On the other hand, our conclusion would be in error if the true filament length distribution in solution were substantially different from that seen in the electron microscope, particularly if many more short filaments were present than were observed.

Even though it is difficult to rationalize the kinetics of subunit exchange in our experiments with the treadmilling model, it is useful for further comparison of our data to those of Wegner to use this model to calculate an apparent actin-monomer flux rate, J_m (μM/h), which is the rate of net monomer incorporation into filaments. This can be done from the slopes of the lines in Fig. 4 that best fit the predicted linear dependence on time for a treadmilling system, the measured critical concentrations (Fig. 2), and Equation 11 (see "Appendix"). The ratio of J_m to the rate of ATP hydrolysis is the measure of kinetic efficiency of an actin treadmill, *i.e.* the number of net monomers incorporated per ATP hydrolyzed. The calculated efficiencies for our experiments are 0.26 in MgCl₂, 0.33 in MgCl₂ + KCl, and about 1.0 in CaCl₂ ± KCl. The flux rate in KCl alone was too low to allow a calculation to be made but if treadmilling occurred at all under this condition it was very inefficient, as also was observed by Wegner and Neuhaus (8). Since we observed tight coupling of ATP hydrolysis to monomer addition during polymerization (Fig. 1), it is reasonable to identify the ATPase rate with the total monomer on-rate, $(k_B^+ + k_P^+)A_1N = (k_B^- + k_P^-)N$, where N is the concentration of filament ends. The kinetic efficiency, within the context of a treadmilling model, would then be equivalent to $J_m/(k_B^- + k_P^-)$, which is the s-value defined originally by Wegner (7). Wegner (7) reported an s-value of 0.25 in MgCl₂ and Wegner and Neuhaus (8) found an s-value of about 1 for an experiment done in CaCl₂; both values are in good agreement with the calculated efficiencies for our experiments under similar conditions.

Furthermore, on the assumption that the measured ATPase rate equals the total monomer on-rate, the sum of the off-rate constants and the sum of the on-rate constants in MgCl₂ can be calculated using the measured critical concentration (A_1

= 2.1 μM) and the concentration of filament ends calculated from the data in Fig. 5 (N = 0.011 μM, average filament length = 2.4 μm). On this basis, the calculated total on-rate constant is k^+ = 1.1 $\times$ 10^5 M^{-1} s^{-1} and the calculated sum of the off-rate constants is k^- = 0.23 s^{-1}. This on-rate constant, calculated from the ATPase rate, is about 100 times larger than the rate constant estimated for polymerization in CaCl$_2$ by Wegner and Engel (2) but is only about 1-2% of the value of the pre-steady state rate constant (k_B^+ + k_P^+) measured directly by electron microscopy, under other buffer conditions, by Pollard and Mooseker (13). Estimations by Tobacman and Korn (3) of the relative elongation rate constants in a variety of polymerization buffers showed that no more than a 10-fold difference can be explained by differences in ionic conditions, and recent preliminary measurements[3] by electron microscopy, under our buffer conditions, give results compatible with those of Pollard and Mooseker. Therefore, the total on-rate constant predicted by the measured ATPase rate and filament length distribution is very much lower than the probable true on-rate constant. This discrepancy could be explained if the filaments were actually about 50 times longer than the measured value, *i.e.* if they were fragmented in the preparative procedures for electron microscopy. Even so, we are still left with the poor fit of the exchange kinetics to the treadmilling model.

As we have already said, however, in contrast to the poor fit of the data to the treadmilling model, our subunit exchange kinetics fit the exchange-diffusion model remarkably well for all the ionic conditions we used. For exchange-diffusion, the rate of labeled subunit incorporation is proportional to $t^{1/2}$ because the small fluctuations that result in the labeling of the terminal subunits occur much more frequently than the larger fluctuations necessary to label further into the filament. Monomer-polymer exchange will go to completion; it just takes a much longer time to do so than we allowed in our experiments. The limited monomer-polymer exchanges we observed in CaCl$_2$ $\pm$ KCl, in KCl alone, and in MgCl$_2$ + KCl (all <10%) agree with the limited exchange measured by Pardee *et al.* (24) in 0.1 M KCl, 1 mM MgCl$_2$, and 1 mM ATP, and the greater exchange we observed in the presence of excess MgCl$_2$ alone (>35%) agrees with the stimulation of exchange in the presence of excess MgCl$_2$ (relative to ATP) reported by Wang and Taylor (25), but not observed by Pardee *et al.* (24). In these previous papers, however, no attempt was made to fit the experimental data to any theoretical model.

When analyzed according to the exchange-diffusion model (Fig. 4; Equation 13, "Appendix"), the slope of the straight lines obtained when $-\ln(F(\infty) - F(t))$ is plotted *versus* $t^{1/2}$ is $(2N/A_1)$ $(k^-/\pi)^{1/2}$. Thus, it is possible to calculate the individual rate constants for exchange-diffusion at the filament ends from the measured critical concentration, A_1, the concentration of filament ends, N, and the exchange data in Fig. 4 without using the ATP hydrolysis data. Assuming that only one end of each filament was rapidly exchanging with the monomer pool, k^+ = 2.8 $\times$ 10^6 M^{-1} s^{-1} and k^- = 5.8 s^{-1} for the experiment in MgCl$_2$ alone. If both filament ends were incorporating subunits at equal rates, both k^+ and k^- would be lower by a factor of 4. These calculated values are in excellent agreement with the pre-steady state rate constants determined by Pollard and Mooseker (13) which were in the range of k^+ = 0.8 - 8.8 $\times$ 10^6 M^{-1} s^{-1} and k^- = 0.7 - 6 s^{-1}, depending on the ionic conditions. As mentioned before, Tobacman and Korn (3) have found that the on- and off-rate constants are not greatly affected by ionic conditions. The agreement between the rate constants calculated from the subunit exchange

data at steady state with the pre-steady state rate constants determined by direct visualization of filament growth provides additional support for the exchange-diffusion model.

However, the k^+ for actin addition calculated from the exchange-diffusion model is about 30-fold higher than that calculated from the steady state ATPase rate, even though ATP hydrolysis and actin monomer addition appear to be tightly coupled during polymerization under these same ionic conditions. These apparently contradictory observations can be rationalized by assuming that there is a segment of actin protomers with bound ATP (instead of ADP) at, at least, one end of the filament. At steady state, addition and loss of a substantial number of actin subunits could then occur without any hydrolysis of ATP. ATP would be hydrolyzed, at steady state, only when addition of an ATP-actin protomer would extend the segment of filament subunits with bound ATP beyond its maximal allowable length. During polymerization, on the other hand, addition events greatly predominate over dissociation events. If the length of the segment that contained bound ATP were to remain constant, each addition during polymerization would necessarily result in the hydrolysis of an ATP bound to an actin protomer further down the filament.

To reconcile the measured rate of ATP hydrolysis at steady state with the kinetics of exchange-diffusion, then, we suggest that addition of an actin monomer to the end of the filament and hydrolysis of that protomer's bound ATP are sequential and separate events. This suggestion had been made previously on theoretical grounds (5) and there is now some independent experimental support for the idea. Recently, Pardee and Spudich (4) reported a lag in the hydrolysis of ATP during polymerization of actin under conditions similar to those in which we (Fig. 1) and others (8) have always observed tight coupling. Also, Mockrin and Korn (26) have shown a substantial uncoupling of ATP hydrolysis from the polymerization of covalently cross-linked actin dimers; in this case, hydrolysis of filament-bound ATP continued for many hours although polymerization was complete in a few minutes. It has previously been demonstrated that the hydrolysis of tubulin-bound GTP can occur subsequent to polymerization (27).

If the hypothesis that segments at the ends of actin filaments contain bound ATP is correct, the measured steady state value of k^- would reflect predominantly the off-rate constant for an F-ATP actin promoter. This could differ significantly from the k^- determined by a dilution-depolymerization experiment which would reflect predominantly the dissociation of F-ADP actin protomers once the short segments of ATP-actin protomers were lost from the filament ends. For similar reasons, it is possible that the experimental data in Fig. 4 fall off the theoretical exchange-diffusion curve at later times because pyrenyl monomer-polymer exchange is being measured in regions of the filament that do not contain bound ATP. Other, possibly slower, reactions would then be needed such as the exchange of ATP for ADP on either the F-actin or G-actin protomer. This would be in addition to any apparent decrease in exchange rate due to the equilibration of short filaments as previously discussed.

On the conventional assumption that the primary exchange reaction at steady state involved the interaction of a G-ATP actin monomer with the filament end and the release of a G-ADP actin monomer from the filament, Neidl and Engel (6) suggested that appreciable G-ADP actin monomers should accumulate in solution because the rate of exchange of ATP for ADP on G-actin is very much slower than the actin dissociation rate. In fact, Tobacman and Korn[4] have been

[3] S. C. Mockrin, S. L. Brenner, and E. D. Korn, unpublished observation.

[4] L. Tobacman and E. D. Korn, unpublished observation.

unable to detect any G-actin with bound ADP in solutions of F- and G-actin at steady state in buffers containing either $MgCl_2$ or KCl. Of course, G-ADP actin would not be expected to be present if the principal reaction were, as we postulate, the exchange of G-ATP actin monomer for F-ATP actin protomers at the filament ends.

We are left, finally, with one major paradox. With a rate constant k^+ of the magnitude measured by Pollard and Mooseker (13) and required to account for our exchange data using the exchange-diffusion model, an actin filament would grow extremely rapidly once nucleation had occurred. For example, with a monomer concentration of 10 μM and a $k^+ = 10^6$ M^{-1} s^{-1}, monomers would add to filaments at an initial rate of 10/ s/filament. At this rate of addition and with the polymerization kinetics described in Fig. 1, the filaments measured in Fig. 5 should have been about 50–100 times longer than the observed values. This paradox can probably be rationalized only by assuming that substantial filament fragmentation occurs either during polymerization or, in the experiments described in Figs. 3–5, when the pyrenyl G-actin was mixed with the preformed F-actin in 0.5 mM $MgCl_2$. Wegner (28) and Wegner and Savko (29) have recently provided evidence for fragmentation during polymerization of actin at low concentrations in solutions containing $MgCl_2$ (and no KCl), but Tobacman and Korn (3) have found no kinetic evidence for significant fragmentation during polymerization in solutions of $MgCl_2$ at the higher actin concentrations used in our experiments.

In summary, it appears that the exchange-diffusion model provides the best explanation for monomer-polymer subunit exchange at steady state under the several experimental conditions that we have used although a number of unanswered questions still remain. Of these, perhaps the most important is the inconsistency between the predicted and measured lengths of actin filaments formed in $MgCl_2$. The discrepancy may be explained by fragility of the filaments but experimental evidence on this point is necessary. Finally, for exchange-diffusion to dominate over treadmilling as the mechanism for monomer-polymer subunit exchange, either the critical concentrations at the two ends of the filaments must be the same (as they may be in KCl (13)) or, if the critical concentrations are different (as they may be in $MgCl_2$ (11, 12)), the magnitude of the rate constants must be very much greater at one end of the filaments than at the other end. Experimental data are also necessary to test these predictions.

Note Added in Proof—After submission of this manuscript, a paper was published by Caplow *et al.* (31) in which they proposed the presence of a short segment of GTP-tubulin subunits at the ends of microtubules analogous to our proposal of a segment of ATP-actin subunits at the ends of microfilaments.

APPENDIX

Monomer-Polymer Subunit Exchange—In steady state monomer-polymer subunit exchange studies performed as described in this paper, all labeled actin monomers are initially in the G-actin pool. Any net incorporation of labeled monomers into F-actin will result in an increase in fluorescence and a decrease in the concentration of labeled G-actin monomers. Initially, the concentration of labeled G-actin monomers is p_0. At a later time, after some exchange has taken place, the concentration of labeled G-actin is p and that the labeled F-actin is $p_0 - p$. The critical monomer concentration remains

constant at A_1. Suppose that there are N filaments/unit volume, at one end of which net replacement of F-actin protomers by G-actin monomers occurs by an unspecified mechanism. When a net exchange of dm monomers between the G-actin and F-actin pools occurs at each of the filament ends, the concentration of labeled G-actin will decrease by an amount dp which is just Ndm times the fraction of the total monomer pool that is labeled, *i.e.*

$$dp = \left(\frac{p}{A_1}\right) \cdot Ndm. \tag{1}$$

Solving Equation 1, we have

$$p(m) = p_0 e^{-Nm/A_1} \tag{2}$$

where $m(t)$, the net number of monomers (both labeled and unlabeled) transferred from monomer pool to polymer pool/ filament, is time-dependent. The concentration of labeled F-actin subunits is just

$$p_0 - p = p_0 (1 - e^{-Nm/A_1}). \tag{3}$$

The measured fluorescence signal $F(t)$ is a sum of the fluorescence from the G-actin and F-actin pools.

$$F = F_G + F_P \tag{4}$$

When all labeled monomers are in the G-actin pool (at $t = 0$), the fluorescence is $F(0)$. Let $F(\infty)$ be the fluorescence expected when all the labeled monomers are in F-actin. It is a property of the pyrenyl actin that $F(\infty)$ is about 25 times $F(0)$ (10).

The fluorescence of the G- and F-actin pools is then just equal to their maximal fluorescence (when all of the label is in that pool) times the fraction of label in the pool at any time,

$$F_G(t) = F(0) \left(\frac{p(m)}{p_0}\right)$$

$$F_P(t) = F(\infty) \left(\frac{p_0 - p(m)}{p_0}\right) \tag{5}$$

Combining Equations 3, 4, and 5 gives

$$F(\infty) - F(t) = (F(\infty) - F(0))e^{-Nm/A_1}. \tag{6}$$

When true fluorescence "equilibrium" is reached, as in the control experiments described above, the label is distributed between the G-actin and F-actin pools and the fluorescence signal is less than $F(\infty)$. The value of $F(\infty)$ can be obtained from the measured fluorescence $F_M(\infty)$ by

$$F(\infty) = \left(\frac{A_T}{A_T - A_1}\right)(F_M(\infty) - F(0)) + F(0) \tag{7}$$

where A_T is the total actin concentration. If $A_T \gg A_1$, essentially all of the label is in F-actin at fluorescence equilibrium and $F(\infty) = F_M(\infty)$.

The fluorescence signal depends on the ratio Nm/A_1, that is the total amount of monomer subunits exchanged with polymer subunits compared to the critical concentration. The fraction of the equilibrium fluorescence observed can be directly calculated from Equation 6 as

$$\frac{F(t) - F(0)}{F_M(\infty) - F(0)} = \left(\frac{A_T}{A_T - A_1}\right)(1 - e^{-Nm/A_1}) \tag{8a}$$

$$= 1 - e^{-Nm/A_1} \quad A_T \gg A_1. \tag{8b}$$

According to Equation 8b, when $Nm = A_1$ we observe 63% of the equilibrium fluorescence; $Nm = 2A_1$ gives 86%; and $Nm = 3A_1$ gives 95% of the final signal. If A_1 represents 5% of the total actin, then only 15% of the F-actin subunits need to exchange to turn over the G-actin pool three times and give 95% of the equilibrium fluorescence. Thus, when most of the

actin monomers are in the F-actin pool, only a small fraction of them need to exchange to observe nearly complete fluorescence equilibrium. To proceed further we must specify the mechanism of subunit exchange, and thereby the time dependence of m.

Treadmilling Model—In a treadmilling model where net subunit incorporation occurs at one polymer end (say the barbed end) and net subunit loss occurs at the opposite (pointed) end we have,

$$m = (k_B^+ A_1 - k_B^-)t = -(k_p^+ A_1 - k_p^-)t \qquad (9)$$

or

$$m = j_m t \qquad (10)$$

where j_m is the (constant) monomer flux rate at each polymer end (monomers/h). Using Equations 10 and 6, we find for a treadmilling system

$$F(\infty) - F(t) = \{(F(\infty) - F(0))e^{-Nj_m t/A_1}. \qquad (11)$$

Therefore, if treadmilling is the primary subunit exchange mechanism, a plot of $-\ln \ (F(\infty) - F(t))$ *versus* t should be linear with a slope Nj_m/A_1.

This formulation for a treadmilling system should be valid until labeled subunits which have been incorporated at the barbed ends of filaments begin to appear at the pointed ends of the same filaments and then get added back to the G-actin pool. Since an F-actin solution contains a distribution of filament lengths (see Fig. 5), there will be a distribution of times at which appearance of label will occur at the pointed ends. The complete solution to this problem requires a precise knowledge of the filament length distribution. We will not attempt to solve the complete problem here (see Ref. 7 for one approach to this problem). By considering a measured filament length distribution, we have shown under "Results" when such considerations should begin to affect significantly the observed exchange data in $MgCl_2$.

Exchange-Diffusion Model—An alternative mechanism by which fluorescent monomers could be incorporated into polymers at steady state is by exchange-diffusion (9). Consider one end of an actin filament at which addition and loss reactions occur at an equal rate so that no treadmilling occurs, i.e. $k^+ A_1 = k^-$. Random fluctuations in the sequence of on- and off-events in this case can result in a net incorporation of labeled monomers into polymers (9, 30). For the special case when all of the monomer pool is labeled at all times, the average distance from the end of a polymer that is labeled is

$$m = 2\left(\frac{k^- t}{\pi}\right)^{1/2} (1 - e^{-k^- t}) \qquad (12a)$$

$$= 2\left(\frac{k^- t}{\pi}\right)^{1/2} \quad t \gg \frac{1}{k^-}. \qquad (12b)$$

Using Equation 6 to correct for the changing concentration of labeled monomers in the G-actin pool, we find

$$F(\infty) - F(t) = (F(\infty) - F(0))\exp\left(-\frac{2N}{A_1}\left(\frac{k^- t}{\pi}\right)^{1/2}\right) \qquad (13)$$

Therefore, a plot of $-\ln \ (F(\infty) - F(t))$ *versus* $t^{1/2}$ should be a straight line if exchange-diffusion is the predominant mechanism of subunit exchange. If both filament ends undergo exchange-diffusion at the same rate, the same equation applies

with N being twice the concentration of F-actin filaments.

Equation 13 must be regarded as an approximation. The full solution has not been obtained to the exchange-diffusion problem with a changing concentration of labeled monomer in the G-actin pool. Notice, however, that the correct equation is recovered for short times, when only a small amount of labeled G-actin has been incorporated into polymer, or when the critical concentration is a high percentage of the total actin. In this case, Equation 12b should apply with label of "fixed" concentration p_0/A_1 incorporated to a depth m on polymers of concentration N. From Equation 3 with $Nm \ll A_1$, we do indeed find that the concentration of labeled F-actin subunits is just

$$p_0 - p(m) = \left(\frac{p_0}{A_1}\right)Nm \qquad (14)$$

REFERENCES

1. Oosawa, F., and Asakura, S. (1975) *Thermodynamics of the Polymerization of Protein*, Academic Press, New York
2. Wegner, A., and Engel, J. (1975) *Biophys. Chem.* **3**, 215–225
3. Tobacman, L., and Korn, E. D. (1983) *J. Biol. Chem.* **258**, 3207–3214
4. Pardee, J. D., and Spudich, J. A. (1982) *J. Cell Biol.* **93**, 648–654
5. Korn, E. D. (1982) *Physiol. Rev.* **62**, 672–737
6. Neidl, C., and Engel, J. (1979) *Eur. J. Biochem.* **101**, 163–169
7. Wegner, A. (1976) *J. Mol. Biol.* **108**, 139–150
8. Wegner, A., and Neuhaus, J.-M. (1981) *J. Mol. Biol.* **153**, 681–693
9. Zeeberg, B., Reid, R., and Caplow, M. (1980) *J. Biol. Chem.* **255**, 9891–9899
10. Kouyama, T., and Mihashi, K. (1981) *Eur. J. Biochem.* **114**, 33–48
11. Brenner, S. L., and Korn, E. D. (1979) *J. Biol. Chem.* **254**, 9982–9985
12. Brenner, S. L., and Korn, E. D. (1980) *J. Biol. Chem.* **255**, 1670–1676
13. Pollard, T. D., and Mooseker, M. S. (1981) *J. Cell Biol.* **88**, 654–659
14. Mockrin, S. C., and Korn, E. D. (1981) *J. Biol. Chem.* **256**, 8228–8233
15. Spudich, J. A., and Watt, S. (1971) *J. Biol. Chem.* **246**, 4866–4871
16. Eisenberg, E., and Kielley, W. W. (1974) *J. Biol. Chem.* **249**, 4742–4748
17. Gordon, D. J., Yang, Y.-Z., and Korn, E. D. (1976) *J. Biol. Chem.* **251**, 7474–7479
18. Lowry, O. H., Rosebrough, N. J., Farr, A. L., and Randall, R. J. (1951) *J. Biol. Chem.* **193**, 265–275
19. Brenner, S. L., and Korn, E. D. (1980) *J. Biol. Chem.* **255**, 841–844
20. Pollard, T. D., and Korn, E. D. (1973) *J. Biol. Chem.* **248**, 4682–4690
21. Pollard, T. D., and Korn, E. D. (1973) *J. Biol. Chem.* **248**, 4691–4697
22. Tellam, R., and Frieden, C. (1982) *Biochemistry* **21**, 3207–3214
23. Pinder, J. C., and Gratzer, W. B. (1982) *Biochemistry* **21**, 4886–4890
24. Pardee, J. D., Simpson, P. A., Stryer, L., and Spudich, J. A. (1982) *J. Cell Biol.* **94**, 316–324
25. Wang, Y.-L., and Taylor, D. L. (1981) *Cell* **27**, 429–436
26. Mockrin, S. C., and Korn, E. D. (1983) *J. Biol. Chem.* **258**, 3215–3221
27. Carlier, M.-F., and Pantaloni, D. (1981) *Biochemistry* **20**, 1918–1924
28. Wegner, A. (1982) *Nature (Lond.)* **296**, 266–267
29. Wegner, A., and Savko, P. (1982) *Biochemistry* **21**, 1909–1913
30. Hill, T. L., and Kirschner, M. (1982) *Int. Rev. Cytol.* **78**, 1–125
31. Caplow, M., Langford, G. M., and Zeeberg, B. (1982) *J. Biol. Chem.* **257**, 15012–15021